Kinetics of the Reaction $NH_2(\tilde{X}^2B_1, v_2 = 0 \text{ and } 1) + NO$

Katsuyoshi Yamasaki,* Akihiro Watanabe,† Aki Tanaka, Manabu Sato, and Ikuo Tokue

Department of Chemistry, Niigata University, Ikarashi, Niigata 950-2181 Japan

Received: August 27, 2001; In Final Form: March 19, 2002

The rate constants for reactions $NH_2(\tilde{X}^2B_1, v_2 = 0 \text{ and } 1) + NO$ have been determined at 298 ± 1 K using the pulsed UV photolysis/pulsed laser-induced fluorescence (LIF) technique. NH_3 was photolyzed with an ArF excimer laser (193 nm), and $NH_2(\tilde{X}^2B_1, v_2 = 0 \text{ and } 1)$ were detected by LIF in the $\tilde{A}^2A_1-\tilde{X}^2B_1$ system. It has been found that CF_4 is efficient at vibrational relaxation of NH_2, and the rate constant for deactivation of $NH_2(\tilde{X}^2B_1, v_2 = 1)$ by CF_4 has been determined to be $[3.2 \pm 0.5(2\sigma)] \times 10^{-11}$ cm^3 molecule^{-1} s^{-1}. Fast vibrational relaxation of NH_2 by CF_4 prior to the reaction with NO permits us to obtain an accurate rate constant for $NH_2(\tilde{X}^2B_1, v_2 = 0) + NO$. The rate constant measured in N_2 buffer gas at 1 Torr is $[2.05 \pm 0.1(2\sigma)] \times 10^{-11}$ cm^3 molecule^{-1} s^{-1}. The sources of discrepancy in previously reported room-temperature rate constants have been discussed on the basis of a survey of the experimental conditions and the methods of analysis. The overall rate constant for $NH_2(\tilde{X}^2B_1, v_2 = 1) + NO$ has been also obtained (without CF_4) to be $[2.6 \pm 0.4(2\sigma)] \times 10^{-11}$ cm^3 molecule^{-1} s^{-1}.

Introduction

The reaction of amidogen (NH_2) with nitrogen monoxide (NO) has attracted the attention of many researchers engaged in atmospheric[1,2] and combustion chemistry.[3,4] Oxidation of ammonia in the atmosphere is initiated by the reaction $OH + NH_3 \rightarrow NH_2 + H_2O$. Because the reactivity of NH_2 with O_2 is very low,[5] the loss of NH_2 is governed by the trace species NO, particularly in the urban areas. Noncatalytic reduction of NO_x by ammonia, called thermal $DeNO_x$ process,[3,6] has been widely used in practical combustion systems, e.g., power plants. The reactions of NH_2 with NO at room-temperature proceeds through the following exothermic channels:

$$NH_2 + NO \rightarrow N_2H + OH \qquad \Delta H^\circ = -4.2 \text{ kJ mol}^{-1} \quad (1a)$$

$$\rightarrow N_2 + H + OH \qquad \Delta H^\circ = -23.8 \text{ kJ mol}^{-1} \quad (1b)$$

$$\rightarrow H_2 + N_2O \qquad \Delta H^\circ = -198.7 \text{ kJ mol}^{-1} \quad (1c)$$

$$\rightarrow N_2 + H_2O \qquad \Delta H^\circ = -522.6 \text{ kJ mol}^{-1} \quad (1d)$$

There have been extensive studies on the rate constants and branching ratios among the channels.[7−40] It is well-known that the overall rate constant shows a negative temperature dependence, and that the reactions proceed via an adduct such as H_2NNO. No production of N_2O was observed by Andresen et al.[15] in the end product analysis, and Silver and Kolb[16] have estimated an upper limit of the branching ratio of reaction 1c to be 0.9% at 300 K. Branching ratios for the processes producing radicals (reactions 1a + 1b) and stable molecules (reaction 1d) have been studied over a wide range of temperatures.[21−26,28,29,31,32,34−40] Most of the studies have reported that the fraction of OH production, $(k_{1a} + k_{1b})/k_1$, is about 0.1 at 298 K and increases with temperature up to 0.4 at 1500 K. There is no experimental report on the detection of N_2H because of its short lifetime (a theoretical study by Phillips[41] predicted the lifetime to be $\sim 10^{-11}$ s at room temperature).

There has been a controversy over the difference between the rate constants measured by the flow method and pulse photolysis. The overall rate constant k_1 for $NH_2(\tilde{X}^2B_1, (0,0,0))$ at room temperature measured by the flow method, approximately 1×10^{-11} cm^3 molecule^{-1} s^{-1},[8,14,16] is smaller than that determined using pulsed photolysis by about a factor of 2.[7,9−11,13,15,17−20,24−26,28,30−33,35,37] There is another unresolved discrepancy in the rate constants measured by pulsed methods at room temperature. A variety of techniques have been employed for pulsed production of NH_2: UV photolysis with ArF (193 nm) laser,[15,18,24,26,30−33,35,37] infrared multiphoton dissociation with CO_2 laser,[19,20] flash photolysis,[9−11,13,17,25] and pulse radiolysis.[7,28] For the past decade, the rate constants k_1 at room temperature reported by some groups are within $(1.4-1.5) \times 10^{-11}$ cm^3 molecule^{-1} s^{-1},[20,30,31,35] and others have given $(1.8-2.2) \times 10^{-11}$ cm^3 molecule^{-1} s^{-1}.[24,26,28,32,33,37] The difference seems to be small compared to commonly accepted errors of reaction rate constants. However, there has been no sign of convergence of the reported rate constants.

In the present study, pulsed laser photolysis of NH_3 followed by the detection of NH_2 via laser-induced fluorescence (LIF) is employed to determine the rate constant for $NH_2(\tilde{X}^2B_1, v_2 = 0 \text{ and } 1) + NO$ reactions. Vibrational levels $(v_1,v_2,v_3) = (0,0,0)$ and (0,1,0) are hereafter represented by $v_2'' = 0$ and $v_2'' = 1$, respectively. Bulatov et al.[25] have shown that the decay rates of NH_2 decrease with an increase in NH_3 concentration. By their careful experiments, Wolf et al.[32,37] have also found that higher concentration of precursor (NH_3) and fluence of photolysis laser are likely to give smaller rate constants. We, therefore, have performed experiments at precursor pressures ($P_{NH_3} < 13$ mTorr) and photolysis laser fluence (<300 μJ cm^{-2}) as low as possible.

* Author to whom correspondence should be addressed. Fax: +81-25-262-7530. E-mail: yam@scux.sc.niigata-u.ac.jp.

† Department of Applied Chemistry, Kobe City College of Technology, Gakuen-Higashi-machi, Nishi-ku, Kobe, 651-2194, Japan.

10.1021/jp013306g CCC: $22.00
Published on Web 06/21/2002

Vibrationally excited NH_2 is produced in the photolysis of NH_3[42−44] and, as a consequence, the profiles of $NH_2(v_2'' = 0)$ do not show a single-exponential decay until vibrational motion is thermalized. Unfortunately, high buffer pressure ($P_{total} > 10$ Torr) is not suitable for detecting $NH_2(\tilde{X}^2B_1)$ by the LIF technique, because electronically excited $NH_2(\tilde{A}^2A_1)$ has a large cross section for quenching even by rare gases.[9,45−47] Therefore, the addition of molecules effective in vibrational relaxation of NH_2 is necessary for measuring an accurate rate constant of $NH_2(v_2'' = 0) + NO$. We have found that CF_4 efficiently accelerates vibrational relaxation of NH_2, and an addition of CF_4 to the system allows us to give an accurate rate constant for the reaction $NH_2(v_2'' = 0) + NO$.

In addition to reaction of the $v_2'' = 0$ level, the overall rate constant for $NH_2(v_2'' = 1) + NO$ has also been determined. A small increase compared to the rate constant for $NH_2(v_2'' = 0) + NO$ was observed.

Experimental Section

Because the experimental apparatus used in the present study has been described previously,[48] only significant features of the present study are described here. Photolysis of NH_3 at 193 nm was employed to generate NH_2. An ArF excimer laser (Lambda Physik LEXtra50) was operated at 20 Hz. It is well-known that not only the electronic ground state $\tilde{X}^2B_1$ but also the excited state $\tilde{A}^2A_1$ is produced in the photolysis of NH_3 at 193 nm.[42,46,49] Branching ratios for the production of these electronic states have not been well established. Donnelly et al.[42] have reported the production yield of $\tilde{A}^2A_1$ state to be about 2.5% from a measurement of fluorescence intensity. Biesner et al.,[49] on the other hand, have given the yield of $\tilde{A}^2A_1$ to be 26 ± 4% using the technique of H atom photofragment translational spectroscopy, claiming that the yield of 2.5% by Donnelly et al. might be a result of the difficulties associated with detection of the fluorescence from $NH_2(\tilde{A}^2A_1)$ fragments in low vibrational states. Because $NH_2(\tilde{A}^2A_1)$ is efficiently quenched even by rare gases,[45,47] $NH_2(\tilde{A}^2A_1)$ produced in the photolysis does not disturb the observation of the reaction between $NH_2(\tilde{X}^2B_1)$ and NO.

The LIF of NH_2 was excited with a Nd^{3+}:YAG laser (Continuum YG660-20) pumped dye laser (Lambda Physik LPD3001 with DCM or C-522 dye). The DCM and C-522 dyes were pumped at 532 and 355 nm lights from the YAG laser, respectively. Vibrational states $NH_2(v_2'' = 0$ and 1) were detected by LIF excited via the 2_0^3 (628 nm) or 2_0^5 (515 nm) and 2_1^6 (532 nm) bands in the $\tilde{A}^2A_1-\tilde{X}^2B_1$ system[50−55] (bent notation for vibrational numbering of the $\tilde{A}^2A_1$ state is adopted here). Vibrational levels 2^3, 2^5, and 2^6 are (0,8,0)Π, (0,12,0)Π, and (0,13,0)Σ, respectively, in linear notation). Typical dye laser fluence was 20−40 μJ pulse^{-1}. Fluorescence from NH_2 was detected with a photomultiplier (Hamamatsu R-374) through optical filters (HOYA R-62 and C-500S). Additional filters (Toshiba ND-50 and ND-10, transmittance at 628 nm was 4.6%) were used to reduce scattered light signal in excitation via the 2_0^3 band. The approximate concentration of initially prepared NH_2 can be estimated to be $\approx 1 \times 10^{12}$ cm^{-3} from the energy density of the photolysis laser at the entrance window of the reaction cell (0.3 mJ cm^{-2}), the photoabsorption cross section of NH_3: $\sigma(193\ nm) = 1.12 \times 10^{-17}$ cm^2,[24] and a typical pressure of NH_3 (13 mTorr). Wolf et al.[32,37] have shown that formation of NH via multiphoton dissociation of NH_3 at 193 nm can be avoided using laser energy density less than 3 mJ cm^{-2}; thus, no significant NH should be produced in the present study.

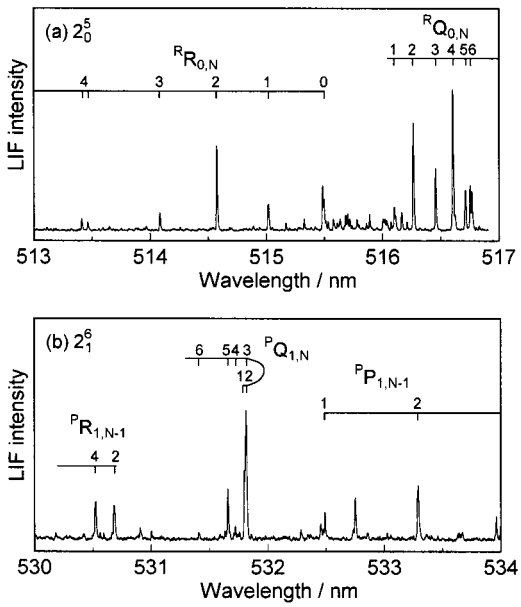

Figure 1. Laser-induced fluorescence excitation spectra of $NH_2(\tilde{X}^2B_1)$ produced in the photolysis of NH_3 at 193 nm: (a) 2_0^5 and (b) 2_1^6 bands in the $\tilde{A}^2A_1-\tilde{X}^2B_1$ system. $P_{NH_3} = 13$ mTorr and $P_{total} = 1$ Torr (N_2). Delay times between the photolysis and probe lasers are (a) 100 μs and (b) 80 μs.

When time-dependent profiles of vibrational levels of interest were recorded, the wavelength of the dye laser was tuned to rotational lines (typically, $^RR_{0,2}$ of 2_0^3 and 2_0^5 bands and $^PQ_{1,N=1-3}$ of 2_1^6 band) and time delay between the photolysis and probe laser was scanned with a homemade delay generator with a step size of 200−400 ns. The number of data points in a profile was at least 1000. After fast rotational relaxation, the intensities of rotational lines are in proportion to the population in a vibrational level of interest.

The flow rates of all the sample gases were controlled with calibrated mass flow controllers (Tylan FC-260KZ and STEC SEC-400 mark3) and mass flow sensors (KOFLOC 3810). Linear flow velocity was 1 m s^{-1}. Total pressure (N_2 buffer, 1 Torr) was monitored with a capacitance manometer (Baratron 122A). The total pressure measurement together with the mole fractions as measured by the flow controllers gave the partial pressures of the reagents.

Highly pure grade NH_3 (Nihon-Sanso, 99.999%), NO (Takachiho Kagaku Cogyo, 99.9%), $NO_2 < 10$ ppm), CF_4 (> 99.99%), and N_2 (Nihon-Sanso, 99.9999%) were used without further purification.

Results and Discussion

Vibrational Relaxation of $NH_2(v_2'' = 1)$ by CF_4. Figure 1, a and b, shows the LIF excitation spectra of $NH_2(v_2'' = 0$ and 1) produced in the NH_3/193 nm photolysis at a total pressure of 1 Torr (N_2). The rotational assignment is based on the previously reported spectroscopic data.[50−55] Time-dependence of the population of the level $v_2'' = 0$ as a function of NO pressures must be measured to determine the rate constant for the reaction $NH_2(v_2'' = 0) + NO$. However, analysis of the time profiles of $v_2'' = 0$ is difficult, when vibrational relaxation ($v_2'' = 1 \rightarrow v_2'' = 0$) by NO occurs simultaneously with the $NH_2(v_2'' = 0) + NO$ reaction. Therefore, a buffer gas having a large cross section for vibrational relaxation of NH_2 must be introduced to thermalize vibrational motion prior to the reaction $NH_2(v_2'' = 0) + NO$. Unfortunately, vibrational relaxation by normally used buffer gases, e.g., rare gases and N_2, is not so

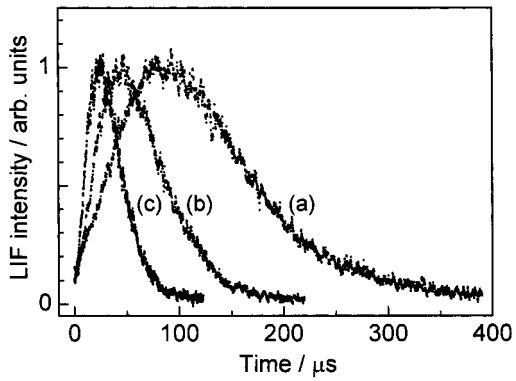

Figure 2. Time profiles of LIF intensities of $NH_2(v_2'' = 1)$ at various CF_4 pressures: $P_{CF_4} = 0$ mTorr, (a); 10 mTorr, (b); and 40 mTorr, (c). $P_{NH_3} = 13$ mTorr and $P_{total} = 1$ Torr (N_2). The abscissa corresponds to the delay time between the photolysis laser and probe laser pulse. All the profiles are so scaled to make their peak intensities the same.

fast: $\approx 10^{-14}-10^{-13}$ cm^3 molecule^{-1} s^{-1}.[44,56,57] No additional gas for accelerating relaxation of NH_2 was used in the previous kinetic studies on NH_2 + NO. Stephens et al.[29] have added SF_6 to enhance relaxation of NH_2 and product H_2O; however, they have only determined branching ratios between the products. Hall et al.[21] have also determined the branching ratios; they have added SF_6 to the system to relax H_2O product. Pagsberg et al.[28] have used 28.5 Torr of SF_6 not for NH_2 relaxation but for producing F atoms in pulse radiolysis.

Chichinin et al.[58] have reported the deactivation rate constant of $ND_2(v_2'' = 1)$ by CF_4: $(1.9 \pm 0.4) \times 10^{-11}$ cm^3 molecule^{-1} s^{-1}, and concluded that the value is typical for a quasi-resonant energy transfer. There is no report on the rate constant for relaxation of $NH_2(v_2'' = 1)$ by CF_4; thus, we have first measured the rate constant for relaxation of $NH_2(v_2'' = 1)$ by CF_4. Figure 2 shows the time profiles of $NH_2(v_2'' = 1)$ at different CF_4 pressures. The time axis is the delay between the photolysis and probe laser pulse. There are 2000 points per time scan, and a single data point represents averaged signals from 10 laser pulses. The decay in the profiles corresponds to vibrational relaxation from $v_2'' = 1$ to $v_2'' = 0$. Although NH_3 is an efficient collider for relaxation ($(4.7 \pm 0.6) \times 10^{-11}$ cm^3 molecule^{-1} s^{-1} [59]), a discernible population of $NH_2(v_2'' = 1)$ is present even at 300 μs after the photolysis under the conditions with no CF_4 (Figure 2a). It is apparent, as shown in Figure 2, b and c, that CF_4 efficiently accelerates the relaxation (decay) of $NH_2(v_2'' = 1)$, and that 40 mTorr of CF_4 depopulates vibrationally excited states within 100 μs. It should be noted that not only the decay but also the growth in the profiles shown in Figure 2 is accelerated by the addition of CF_4. The growth in the profiles reflects rotational relaxation from highly excited rotational levels of $v_2'' = 1$ to a detected rotational level, and the following vibrational relaxation from the levels of $v_2'' \geq 2$. Nadtochenko et al.[44] have reported that 75 $\pm$ 10% of NH_2 are vibrationally excited, and Biesner et al.[49] have also shown that highly excited vibrational and rotational levels of NH_2 are generated in the photolysis of NH_3 at 193 nm.

Pseudo-first-order conditions ($[NH_2]_0 \ll [CF_4]$) are satisfied in the present study, and consequently, the first-order rates governing the profiles are linearly dependent on $[CF_4]$. Initially populated vibrational levels higher than $v_2'' = 1$ cascade down to $v_2'' = 1$ by collisions of CF_4 as shown in the following scheme:

$$v \xrightarrow{k_v[CF_4]} v-1 \xrightarrow{k_{v-1}[CF_4]} \cdots\cdots \xrightarrow{k_2[CF_4]} v_2 = 1 \xrightarrow{k_1[CF_4]}$$

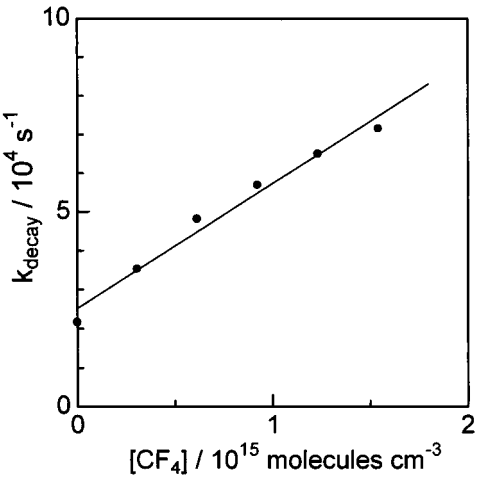

Figure 3. Plot of apparent first-order decay rate of $NH_2(v_2'' = 1)$ versus CF_4 concentrations. k_{decay} is obtained from semilogarithmic analysis of the time profiles as shown in Figure 2. The slope of the straight line fit from regression analysis gives a deactivation rate constant of $NH_2(v_2'' = 1)$ by CF_4: $[3.2 \pm 0.5(2\sigma)] \times 10^{-11}$ cm^3 molecule^{-1} s^{-1}.

An analytical expression of the concentration profile of $v_2'' = 1$ is given by the following multiple exponential form:[60]

$$[v_2 = 1] = C_v e^{-k_v[CF_4]t} + C_{v-1}e^{-k_{v-1}[CF_4]t} + \cdots + C_2 e^{-k_2[CF_4]t} + C_1 e^{-k_1[CF_4]t} \quad (2)$$

where C_i are constants related to the initial vibrational populations and rate constants. In general, higher vibrational levels relax faster than lower levels, i.e., $k_v > k_{v-1} > \ldots > k_2 > k_1$. The last two terms, $C_2e^{-k_2[CF_4]t} + C_1e^{-k_1[CF_4]t}$, are predominant over other terms after an appropriate delay time t_1, and profiles after the initial t_1 can be fitted to a double exponential form. However, t_1 cannot be determined without the values of relaxation rate constant of the levels $v_2'' \geq 2$. This is the case for the present study, and single-exponential analysis was made as an alternative way. Time profiles of $v_2'' = 1$ are governed only by the last term $C_1e^{-k_1[CF_4]t}$ after the delay time t_2. For example, t_2 for the profiles shown in Figure 2 are 180, 110, and 55 μs for a, b, and c, respectively. Semilogarithmic analysis of the time profiles after t_2 gives apparent first-order decay rate constants k_{decay}. Figure 3 shows a plot of k_{decay} versus CF_4 concentrations. The slope corresponds to a rate constant for deactivation of $NH_2(v_2'' = 1)$ by CF_4: $[3.2 \pm 0.5(2\sigma)] \times 10^{-11}$ cm^3 molecule^{-1} s^{-1}. The error originates mainly from statistical deviation of semilogarithmic analysis and the scatter of the data shown in Figure 3. The intercept of the plot represents the sum of the rates of relaxation by NH_3 and N_2 and diffusion loss from the volume probed with the dye laser.

Deactivation rates of ND_2 and NH_2 by CF_4 are surprisingly fast. All the reported rate constants for deactivation of NH_2 by molecules having neither polarity nor N$-$H bonds are less than 1×10^{-12} cm^3 molecule^{-1} s^{-1}.[44,56-58] Vibrational energies of $NH_2(v_2'' = 1)$ and $ND_2(v_2'' = 1)$ are 1497 cm^{-1} and 1109 cm^{-1},[61] respectively; vibrational quanta of CF_4 are 909 cm^{-1} (ν_1), 435 cm^{-1} (ν_2), 1281 cm^{-1} (ν_3), and 632 cm^{-1} (ν_4).[62] Assuming that deactivation of $ND_2(v_2'' = 1)$ and $NH_2(v_2'' = 1)$ by CF_4 proceeds via a V$-$V mechanism,[58] vibrational energy of $ND_2(v_2'' = 1)$ 1109 cm^{-1} is transferred to ν_1 and/or ν_3 vibrations of CF_4, and $NH_2(v_2'' = 1)$ 1497 cm^{-1} to ν_3 of CF_4 as follows:

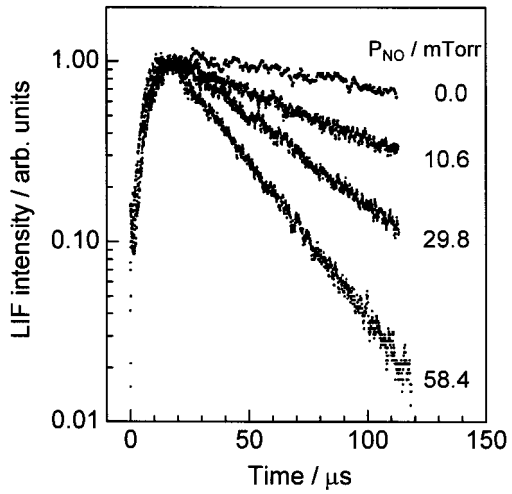

Figure 4. Semilogarithmic plots of the time profiles of $NH_2(v_2'' = 0)$ at various NO pressures. The time axis is the delay between the photolysis and probe laser. $P_{NH_3} = 13$ mTorr, $P_{CF_4} = 240$ mTorr, and $P_{total} = 1$ Torr (N_2).

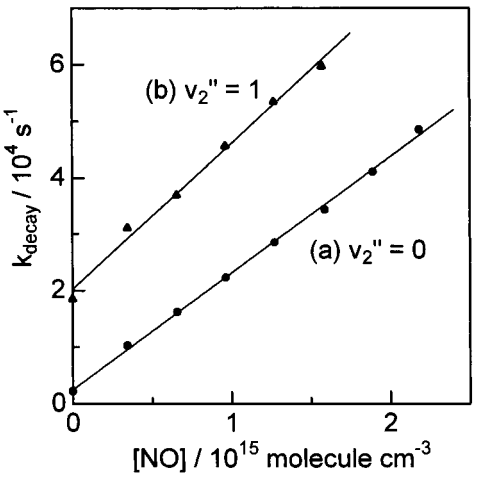

Figure 5. Plot of apparent first-order decay rate of $NH_2(v_2'' = 0$ and 1) versus NO concentrations. The slopes of the straight lines fit by regression analysis give overall rate constant for $NH_2(v_2'' = 0)$ + NO: $[2.05 \pm 0.1(2\sigma)] \times 10^{-11}$ cm^3 molecule^{-1} s^{-1}, and $NH_2(v_2'' = 1)$ + NO: $[2.6 \pm 0.4(2\sigma)] \times 10^{-11}$.

$$ND_2(v_2'' = 1) + CF_4 \rightarrow ND_2(v_2'' = 0) + CF_4(v_1 = 1) + 200\ cm^{-1} \quad (3a)$$

$$ND_2(v_2'' = 1) + CF_4 \rightarrow ND_2(v_2'' = 0) + CF_4(v_3 = 1) - 172\ cm^{-1} \quad (3b)$$

$$NH_2(v_2'' = 1) + CF_4 \rightarrow NH_2(v_2'' = 0) + CF_4(v_3 = 1) + 216\ cm^{-1} \quad (4)$$

The magnitudes of energy defects are almost identical for these processes; nevertheless, deactivation of $NH_2(v_2'' = 1)$ by CF_4 is faster than that of $ND_2(v_2'' = 1)$ by CF_4 by a factor of 1.7.

Rate Constants for Reactions of $NH_2(v_2'' = 0$ and 1) + NO. Because CF_4 has been found to be an effective collider for vibrational relaxation of NH_2, a large amount of CF_4 (240 mTorr) was added to the system for measuring the reaction rates of reaction $NH_2(v_2'' = 0)$ + NO. Semilogarithmic plots of the LIF intensities of $NH_2(v_2'' = 0)$ as a function of reaction time at various NO pressures are shown in Figure 4. Profiles reach their maxima at about 20 μs, although the estimated time constant of vibrational relaxation of $v_2'' = 1$ by 240 mTorr of CF_4 is 4 μs. The difference gives an evidence that higher vibrational levels than $v_2'' = 1$ are produced in the photolysis of NH_3 at 193 nm and relaxed to $v_2'' = 0$ via $v_2'' = 1$. The cascade of vibrational levels makes the times for maximum intensities longer than those estimated from only the relaxation rate constant for $v_2'' = 1$.

There are several possible disproportionation and recombination reactions of NH_2:

$$NH_2 + NH_2 \rightarrow HN{=}NH + H_2 \quad (5a)$$

$$\rightarrow NH + NH_3 \quad (5b)$$

$$\rightarrow NH_2NH + H \quad (5c)$$

$$(+ N_2) \rightarrow N_2H_4\ (+ N_2) \quad (5d)$$

Reported rate constants for these reactions are $k_{5a}(300\ K) = 1.3 \times 10^{-12}$ cm^3 molecule^{-1} s^{-1},[63] $k_{5b}(298\ K) = 7.64 \times 10^{-13}$ cm^3 molecule^{-1} s^{-1},[64] $k_{5c}(300\ K) < 1 \times 10^{-13}$ cm^3 molecule^{-1} s^{-1},[63] and $k_{5d}(298\ K) = 6.89 \times 10^{-30}$ cm^6 molecule^{-2} s^{-1}.[65] Here, we have chosen the fastest values reported so far to evaluate the upper limits of the effects by these background reactions. Time constants for reactions 5a−5d are calculated to be 0.8 s, 1.3 s, >10 s, and 4.5 s, respectively, from the present experimental conditions ($[NH_2]_0 \approx 1 \times 10^{12}$ molecule cm^{-3} and $P_{total} = 1$ Torr (N_2)). Because the time constant of the $NH_2(v_2'' = 0)$ + NO reaction is an order of 10^{-4} s even at the lowest NO concentration in the present study (10.6 mTorr), all the above background reactions must be negligibly slow as can be seen in Figure 4 at $P_{NO} = 0$.

Regeneration of NH_2 is possible by the following reaction:

$$OH + NH_3 \rightarrow NH_2 + H_2O \quad (6)$$

Since the hydroxyl radical OH is produced in NH_2 + NO reactions (reactions 1a or 1b). The rate constant for reaction 6, 1.6×10^{-13} cm^3 molecule^{-1} s^{-1},[5] corresponds to a time constant 1.5×10^{-2} s which is 150 times longer than the time scales of observed NH_2 + NO reactions. Therefore, any background reactions related to regeneration of NH_2 can be assumed to be negligible under the present experimental conditions.

All the plots in Figure 4 show straight lines after 30 μs, which indicates that the population of the level $v_2'' = 1$ is negligibly small after the initial 30 μs. This is in contrast to the observation that a discernible population of $v_2'' = 1$ is present even after 300 μs under the same conditions, except for the absence of CF_4 (Figure 2a). The ratios of $[NO]/[NH_2]_0$ are always larger than 230, and the pseudo-first-order conditions are satisfied. The first-order decay rate constants were obtained by the analysis of the decays after the initial 35 μs. The dependence of the decay rates on NO pressures is shown in Figure 5a, giving the rate constant for the reaction between $NH_2(v_2'' = 0)$ and NO to be $[2.05 \pm 0.1(2\sigma)] \times 10^{-11}$ cm^3 molecule^{-1} s^{-1}. The error is due mainly to the scatter in the data points of the plot and the uncertainties of pressures of reagents.

Reported rate constants for $NH_2(v_2'' = 0)$ + NO reaction at room temperature are listed in Table 1 in chronological order. There is no systematic change in the rate constant with total pressure (0.1−760 Torr) and buffer gases (He, Ar, N_2, and O_2). A significant feature is that rate constants measured by discharge-flow method[8,14,16] are smaller than those obtained using pulsed photolysis by about a factor of 2. The discrepancy has been a source of controversy for a long time. Jeffries et

TABLE 1: Rate Constants for the Reaction $NH_2(v_2 = 0)$ + NO at Room Temperature

k^a	$[NH_3]/cm^{-3}$	$[NH_2]_0/cm^{-3}$	method[b]	P_{total}/Torr	buffer	T/K	refs
2.7	$8 \times 10^{15}-5 \times 10^{19}$		PR/PA	250−1520		298	7
0.83 ± 0.17	8×10^{15}	$\approx 2 \times 10^{14}$	DF/MS	1−10	He	298	8
2.1 ± 0.2	3.2×10^{15}	$<6.4 \times 10^{10}$	FP/CWLIF	0.9	Ar	298	9
1.8 ± 0.3	1×10^{17}	$6 \times 10^{13}-1.8 \times 10^{14}$	FP/PA	2−700	N_2	300	10
1.7 ± 0.4	$3.3 \times 10^{14}-3.3 \times 10^{15}$	$<3.3 \times 10^{12}$	FP/LA	0.1−1	Ar	293	11
1.9 ± 0.2	$6.4 \times 10^{14}-1.6 \times 10^{16}$	10^8-10^9	FP/CWLIF	3−10	He	298	13
1.2	$1.7 \times 10^{13}-6.6 \times 10^{15}$	$<1.6 \times 10^{13}$	DF/CWLIF	0.6−4	He	298	14
1.7 ± 0.5	$6 \times 10^{13}-6 \times 10^{15}$		UVLP/PA, LIF, IREM		He	295	15
0.9		$<5 \times 10^{11}$	DF/LIF,RF	1.15−1.51	He	298	16
2.10 ± 0.62^c	3.2×10^{15}		FP/CWLIF	2.5−10	Ar	298	17
1.81 ± 0.12^c	3×10^{14}		UVLP/LIF	1−2	He	297	18
0.90	1×10^{14} [d]	$<3 \times 10^{11}$	IRLP and flow/LIF, RF, MS	1	He	r.t.[f]	19
1.4 ± 0.1	$<1.6 \times 10^{15}$ [e]		IRLP/LIF	2−5.5	Ar	298	20
2.0 ± 0.4	$(0.16-32.2) \times 10^{16}$	$\approx 3 \times 10^{12}$	FP/LA	10	N_2	298	25
1.8 ± 0.2	$\approx 4 \times 10^{14}$		UVLP/LIF	10	N_2	294	24, 26
2.2 ± 0.3	$\approx 10^{17}$		PR/PA	760	Ar	298	28
1.45 ± 0.15^c	$(1.3-4.4) \times 10^{15}$	$(1-5) \times 10^{12}$	UVLP/CRD	50, 60	Ar	297	30, 31
1.9 ± 0.3^c	$<1.3 \times 10^{13}$	$(2-3) \times 10^{11}$	UVLP/MS	6	O_2	299	33
1.46 ± 0.15^c	$\approx 2.1 \times 10^{15}$	$\approx 1.8 \times 10^{14}$	UVLP/MS	4.3−5.2	He	305	35
1.9 ± 0.1^c	$1.2 \times 10^{14}-1.9 \times 10^{14}$	$\approx 4 \times 10^{12}$	UVLP/CWLIF	10	Ar	295	32, 37
2.05 ± 0.1^c	4×10^{14}	$<1 \times 10^{12}$	UVLP/LIF	1	N_2	298	this work

[a] In units of 10^{-11} cm^3 molecule^{-1} s^{-1}. [b] PR: pulse radiolysis; DF: discharge flow; FP: flash photolysis; UVLP: UV laser photolysis (193 nm); IRLP: infrared laser photolysis; PA: Photoabsorption; MS: mass spectrometry; CWLIF: continuous wave laser-induced fluorescence (LIF); LA: intracavity laser absorption; IREM: infrared emission; RF: resonance fluorescence; LIF: pulsed LIF; CRD: cavity-ring-down method. [c] Denoted errors are 2σ. [d] Precursor is N_2H_4. [e] Precursors are N_2H_4 and CH_3NH_2. [f] Room temperature.

al.[19] produced NH_2 using infrared laser decomposition in a dissociator cell, and then introduced NH_2 to a flow cell for observing NH_2 + NO reaction. They produced NH_2 with a pulse laser; nevertheless, their rate constant, 9×10^{-12} cm^3 molecule^{-1} s^{-1}, is almost identical with the averaged value given by the flow method. Whyte and Phillips[18] have pointed out that long-lived NH_2NO adduct diffuses out of the observation region in a photolysis method, but redissociates to NH_2 + NO in an observation time scale typical of a flow tube method. However, this explanation seems implausible, because the observation times of experiments of refs 17 (3 ms) and 33 (8 ms), which employed pulsed photolysis and reported large rate constants, are not much shorter than those of flow method.

The small rate constants given by the discharge-flow methods might be due to the plug-flow assumption made in the analysis. Howard[66] has pointed out that the flow methods are likely to give considerably small rate constants unless the concentration gradient of reactants in a flow tube is carefully corrected. Specifically, when homogeneous and wall-depletion rates are large, conversion from axial distance to reaction time cannot be made. Dorthe et al.[67] have shown that plug-flow rate constant values are significantly smaller than those given by the solution of the differential continuity equation. They have measured rate constants for the reactions of atomic carbon with OCS and NO, demonstrating that the rate constants obtained on the plug-flow assumption are about 1.6 times smaller than those determined by the continuity equation. The homogeneous and wall removal rate constants in their measurements were $\sim 10^{-11}-10^{-10}$ cm^3 molecule^{-1} s^{-1} and $\sim 10^2$ s^{-1}, respectively, and these values are similar to those in the case of NH_2 + NO reactions.[16] Of the studies on NH_2 + NO reaction using flow tube methods, Silver and Kolb[16] corrected for the effects of axial and radial diffusion in their analysis; however, they determined the rate constants on the assumption that reaction time can be calculated from axial distance.

Studies using pulsed methods are also divided into two groups: one group has reported rate constants of $(1.4-1.5) \times 10^{-11}$ cm^3 molecule^{-1} s^{-1},[20,30,31,35] and the other of $(1.7-2.2) \times 10^{-11}$ cm^3 molecule^{-1} s^{-1}.[24,26,28,32,33,37] Although this difference is not so large, no convergence has been made.

Stephens et al.[29] have suggested that high NH_3 concentrations and photolysis result in thermal shock waves because of a large energy release of the reaction 1d. They have calculated that the temperature rise is between 5 and 10 K, depending on the pulse energy and NH_3 concentration. Because the rate constant of NH_2 + NO shows a negative temperature dependence, a slightly smaller rate constant is obtained. However, a decrease in rate constants estimated from the temperature rise is less than 5% that is too small to account for the underestimation of rate constants measured at high NH_3 concentrations. By their systematic check, Wolf et al.[32,37] have found that higher concentrations of NH_3 and photolysis energies lead to smaller rate constants, and that lowering NH_3 and/or photolysis energies did not further change the measured rate constants. Indeed all the measurements giving small rate constants[20,30,31,35] were made at high NH_3 concentrations, but Wolf et al. have not given a decisive reason for the decrease in rate constants measured at high NH_3 pressures and photolysis energies. Bulatov et al.[25] have also observed an apparent decrease in rate constants at high NH_3 pressures, and concluded that the cause is regeneration of NH_2 by OH + $NH_3 \rightarrow NH_2 + H_2O$ following reactions 1a and 1b. It has been established that the yield of OH in the NH_2 + NO reaction is about 10% at room temperature.[37,40] Therefore, the amount of regenerated NH_2 by OH + NH_3 is not large enough to account for the small rate constants at high NH_3 and/or NH_2 concentrations.

Here we discuss the other possible causes of the small rate constants. Gericke et al.[20] added a large amount of NO (maximum pressure was 3 Torr). The addition of NO accelerates not only chemical reactions of $NH_2(v_2'' = 0)$ + NO but also vibrational relaxation and/or reaction of $NH_2(v_2'' = 1)$ with NO. As a consequence, both rates for the growth and decay of $NH_2(v_2'' = 0)$ are increased. They used 50 mTorr of CH_3NH_2 as a precursor of NH_2, and added 2 Torr of Ar to suppress diffusion loss of NH_2. In their experiments, the first-order rates of total removal of $v_2'' = 1$ by CH_3NH_2 and Ar, which are estimated to be 1.2×10^5 s^{-1} and 1.9×10^4 s^{-1} from previously reported rate constants,[20,57,59] are much smaller than 1.5×10^6 s^{-1} for the removal at a typical pressure (1.5 Torr) of NO. Therefore, It might be difficult to eliminate the effect of growth

lowering the apparent rates of $NH_2(v_2'' = 0)$ + NO reaction. Unfortunately, neither temporal profiles nor semilogarithmic plots of $NH_2(v_2'' = 0)$ are shown in their paper, and the details of their analysis are unclear. NO accelerates both growth and decay of the profiles of $NH_2(v_2'' = 0)$ also in the present study. However, the increase in the rates of growth on addition of NO is negligibly small, because the growth of $v_2'' = 0$ is totally governed by 240 mTorr of CF_4 in the present experiments (see Figure 4). Another problem of their measurement is time resolution. A large amount of NO was added, and apparent time constant of the reaction of interest was about 700 ns at the highest NO pressure. They recorded a profile with 512 points per scan, and thus an interval of data points was 1.4 ns. However, the pulse duration of their probe laser (N_2 laser pumped dye laser) was about 8 ns. The fact suggests that effective time resolution was too poor to derive an accurate rate constant.

Park and Lin[35] employed UV laser photolysis coupled with pinhole sampling using electron impact mass spectrometry. They did not detect NH_2, but observed time-resolved concentration profiles of NO and H_2O, and gave a relatively small rate constant $(1.46 \pm 0.15) \times 10^{-11}$ cm^3 molecule^{-1} s^{-1} at 305 K. Detection by mass spectrometry differs from that of laser-based techniques in state selectivity. If rate constants for the reactions $NH_2(v_2'' \geq 1)$ + NO are different from that for $NH_2(v_2'' = 0)$ + NO, then rate constants measured by mass and laser detection techniques may be different. However, Imamura and Washida[33] have employed a similar pinhole sampling technique, and directly detected NH_2 by photoionization mass spectrometry at various NO pressures, giving the rate constant to be $(1.9 \pm 0.3) \times 10^{-11}$ cm^3 molecule^{-1} s^{-1} at 299 K. Their rate constant falls into a group of relatively large rate constants. Accordingly, mass detection is not a cause of the discrepancy in the rate constants. A significant difference in the experimental conditions in the two studies is the initial NH_2 concentration: $[NH_2]_0 \approx 1.8 \times 10^{14}$ molecule cm^{-3} in ref 35, and $< 3 \times 10^{11}$ molecule cm^{-3} in ref 33. Park and Lin did not adopt the pseudo-first-order conditions ($0.35 \leq [NO]/[NH_2]_0 \leq 0.93$ in measurement at 305 K), and they were not able to neglect the competing radical−radical reactions. Thus they simulated the kinetics of the system consisting of 71 reactions. Self-reactions of NH_2 (reactions 5a and 5b) and the reaction of NH_2 with H were taken into account as background processes related to the initial products of the photolysis of NH_3. Reliability of the rate constants determined by simulation is strongly dependent on the accuracy of the kinetic data used in calculation. Unfortunately, none of the rate constants for these reactions at around 300 K have been established. The rate constant of reaction 5a used in the simulation was 8.3×10^{-13} cm^3 molecule^{-1} s^{-1};[68] Stothard et al.[63] have reported a larger rate constant to be 1.3×10^{-12} cm^3 molecule^{-1} s^{-1}. There is a large discrepancy among reported rate constants of reaction 5b measured at room temperature: $1.15 \times 10^{-18} - 7.64 \times 10^{-13}$ cm^3 molecule^{-1} s^{-1}.[64,69−71] Rate constants for reactions 5b and NH_2 + H in the simulation were extrapolated using temperature dependence measured by shock tube experiments at 2200−2800 K.[68] Actually, the difference in the rate coefficients for NH_2 + NO reported by Wolf et al. and Park and Lin is smaller at higher temperature. It might be suggested that a little small rate constant for NH_2 + NO reaction determined by the simulation results from incorrect rate constants used.

Diau et al.[31] have measured the rate constant by cavity-ring-down technique at relatively low NH_2 concentration ($(1-5) \times 10^{12}$ cm^{-3}). Their measurements seem to be affected by neither vibrational relaxation nor radical−radical reactions. Nevertheless, they have reported a relatively small rate constant $((1.45 \pm 0.15) \times 10^{-11}$ cm^3 molecule^{-1} s^{-1} at 297 K). The concentration of NH_3 was high, and their result is consistent with the tendency for rate constant to decrease at high NH_3 concentrations as pointed out by Wolf et al.,[32,37] although this is by no means certain.

The overall rate constant for $NH_2(v_2'' = 1)$ + NO has also been determined in the present study. No CF_4 was added in the system when the time profiles of $NH_2(v_2'' = 1)$ were recorded. The growth and decay of the time profiles of $v_2'' = 1$ are accelerated by NO, because the rates of reactions and/or relaxation of $NH_2(v_2'' = 1$ and 2) are linearly dependent on NO concentration. We have, therefore, analyzed time profiles in the range of a long delay time by single-exponential analysis in the same manner as described in the analysis for determining the rate constant of relaxation of $NH_2(v_2'' = 1)$ by CF_4. The potential uncertainty is larger than that for the $NH_2(v_2'' = 0)$ + NO case, because the number of data points used in the analysis is limited. From the dependence of the apparent first-order decay rates versus NO concentrations have given a rate constants for $NH_2(v_2'' = 1)$ + NO to be $[2.6 \pm 0.4(2\sigma)] \times 10^{-11}$ cm^3 molecule^{-1} s^{-1} (Figure 5b). Gericke et al.[20] have also shown the acceleration of total removal of NH_2 upon excitation of bending vibration, whereas their value $((3.2 \pm 0.2) \times 10^{-11}$ cm^3 molecule^{-1} s^{-1}) is larger than ours. There are too many differences in experimental conditions to find the causes of the discrepancy in the rate constants. Gericke et al. decomposed CH_3NH_2 or N_2H_4 with an infrared laser, and added a much larger amount of NO (≤3.5 Torr) than in the present study (≤70 mTorr). They have concluded that the increase in the rate constant upon vibrational excitation is indicative of an acceleration of reactive removal of NH_2 by NO, on the assumption that deactivation rates of $NH_2(v_2'' = 1)$ by NO are not so different from those by O_2 and N_2: $10^{-13}-10^{-12}$ cm^3 molecule^{-1} s^{-1}.[44,56,57] However, there is a possibility that NO shows a larger cross-section for vibrational relaxation than would be expected from results on O_2 and N_2,[72] because NO has a radical character. To determine accurate branching ratios between reactive removal and vibrational relaxation of $NH_2(v_2'' = 1)$ + NO, calibration of detectivities of $NH_2(v_2'' = 0)$ and $NH_2(v_2'' = 1)$ must be made.

Summary

It has been found that CF_4 is an effective collider for vibrational relaxation of NH_2. The deactivation rate constant of $NH_2(v_2 = 1)$ by CF_4 has been determined to be $[3.2 \pm 0.5(2\sigma)] \times 10^{-11}$ cm^3 molecule^{-1} s^{-1}, and it is larger than that for $ND_2(v_2 = 1)$ by CF_4 by a factor of 1.7. The fast relaxation of NH_2 by CF_4 enables us to determine an accurate rate constant for $NH_2(v_2 = 0)$ + NO reaction: $[2.05 \pm 0.1(2\sigma)] \times 10^{-11}$ cm^3 molecule^{-1} s^{-1}. Our rate constant supports the relatively larger rate coefficients around 2×10^{-11} cm^3 molecule^{-1} s^{-1} reported so far for the $NH_2(v_2 = 0)$ + NO reaction. The overall rate constant for $NH_2(v_2 = 1)$ + NO has also been determined: $[2.6 \pm 0.4(2\sigma)] \times 10^{-11}$ cm^3 molecule^{-1} s^{-1}.

Acknowledgment. This work was supported by the Grant-in-Aid for Scientific Research on Priority Areas "Free Radical Science" (Contract No. 05237106), Grant-in-Aid for Scientific Research (B) (Contract No. 08454181), and Grant-in-Aid for Scientific Research (C) (Contract No. 10640486) of the Ministry of Education, Science, Sports, and Culture.

References and Notes

(1) McConnell, J. C. *J. Geophys. Res.* **1973**, *78*, 7812.
(2) Logan, J. A.; Prather, M. J.; Wofsy, S. C.; McElroy, M. B. *J. Geophys. Res.* **1981**, *86*, 7210.
(3) Lyon, R. K. *Int. J. Chem. Kinet.* **1976**, *8*, 315.
(4) Miller, J. A.; Branch, M. C.; Kee, R. J. *Combust. Flame* **1981**, *43*, 81.
(5) DeMore, W. B.; Sander, S. P.; Golden, D. M.; Hampson, R. F.; Kurylo, M. J.; Howard, C. J.; Ravishankara, A. R.; Kolb, C. E.; Molina, M. J. *Chemical Kinetics and Photochemical Data for Use in Stratospheric Modeling*; NASA JPL Publication 97-4; Jet Propulsion Laboratory: California Institute of Technology: Pasadena, 1997.
(6) Lyon, R. K. U. S. Patent 3,900,554 (1975).
(7) Gordon, S.; Mulac, W.; Nangia, P. *J. Phys. Chem.* **1971**, *75*, 2087.
(8) Gehring, M.; Hoyermann, K.; Schacke, H.; Wolfrum, J *Symp. Int. Combust. Proc.* **1973**, *15*, 99.
(9) Hancock, G.; Lange, W.; Lenzi, M.; Welge, K. H. *Chem. Phys. Lett.* **1975**, *33*, 168.
(10) Lesclaux, R.; Khê, P. V.; Dezauzier, P.; Soulignac, J. C. *Chem. Phys. Lett.* **1975**, *35*, 493.
(11) Sarkisov, O. M.; Cheskis, S. G.; Sviridenkov, E. A. *Bull. Russ. Acad. Sci. USSR, Div. Chem. Sci.* **1978**, *27*, 2336.
(12) Roose, T. R.; Hanson, R. K.; Kruger, C. H. *Symp. Int. Shock Tubes Waves Proc.* **1978**, *11*, 245.
(13) Kurasawa, H.; Lesclaux, R. *Chem. Phys. Lett.* **1979**, *66*, 602.
(14) Hack, W.; Schacke, H.; Schröter, M.; Wagner, H. G. *Symp. Int. Combust. Proc.* **1979**, *17*, 505.
(15) Andresen, P.; Jacobs, A.; Kleinermanns, C.; Wolfrum, J. *Symp. Int. Combust. Proc.* **1982**, *19*, 11.
(16) Silver, J. A.; Kolb, C. E. *J. Phys. Chem.* **1982**, *86*, 3240.
(17) Stief, L. J.; Brobst, W. D.; Nava, D. F.; Borkowski, R. P.; Michael, J. V. *J. Chem. Soc., Faraday Trans. 2* **1982**, *78*, 1391.
(18) Whyte, A. R.; Phillips, L. F. *Chem. Phys. Lett.* **1983**, *102*, 451.
(19) Jeffries, J. B.; McCaulley, J. A.; Kaufman, F. *Chem. Phys. Lett.* **1984**, *106*, 111.
(20) Gericke, K.-H.; Torres, L. M.; Guillory, W. A. *J. Chem. Phys.* **1984**, *80*, 6134.
(21) Hall, J. L.; Zeitz, D.; Stephens, J. W.; Kasper, J. V. V.; Glass, G. P.; Curl, R. F.; Tittel, F. K. *J. Phys. Chem.* **1986**, *90*, 2501.
(22) Dolson, D. A. *J. Phys. Chem.* **1986**, *90*, 6714.
(23) Silver, J. A.; Kolb, C. E. *J. Phys. Chem.* **1987**, *91*, 3713.
(24) Atakan, B.; Jacobs, A.; Wahl, M.; Weller, R.; Wolfrum, J. *Chem. Phys. Lett.* **1989**, *155*, 609.
(25) Bulatov, V. P.; Ioffe, A. A.; Lozovsky, V. A.; Sarkisov, O. M. *Chem. Phys. Lett.* **1989**, *161*, 141.
(26) Atakan, B.; Wolfrum, J.; Weller, R. *Ber. Bunsen-Ges. Phys. Chem.* **1990**, *94*, 1372.
(27) Unfried, K. G.; Glass, G. P.; Curl, R. F. *Chem. Phys. Lett.* **1990**, *173*, 337.
(28) Pagsberg, P.; Sztuba, B.; Ratajczak, E.; Sillesen, A. *Acta Chem. Scand.* **1991**, *45*, 329.
(29) Stephens, J. W.; Morter, C. L.; Farhat, S. K.; Glass, G. P.; Curl, R. F. *J. Phys. Chem.* **1993**, *97*, 8944.
(30) Yu, T.; Lin, M. C. *J. Phys. Chem.* **1994**, *98*, 2105.
(31) Diau, E. W.; Yu, T.; Wagner, M. A. G.; Lin, M. C. *J. Phys. Chem.* **1994**, *98*, 4034.
(32) Wolf, M.; Yang, D. L.; Durant, J. L. *J. Photochem. Photobiol. A: Chem.* **1994**, *80*, 85.
(33) Imamura, T.; Washida, N. *Laser Chem.* **1995**, *16*, 43.
(34) Park, J.; Lin, M. C. *J. Phys. Chem.* **1996**, *100*, 3317.
(35) Park, J.; Lin, M. C. *J. Phys. Chem. A* **1997**, *101*, 5.
(36) Glarborg, P.; Kristensen, P. G.; D.-Johansen, K.; Miller, J. A. *J. Phys. Chem. A* **1997**, *101*, 3741.
(37) Wolf, M.; Yang, D. L.; Durant, J. L. *J. Phys. Chem. A* **1997**, *101*, 6243.
(38) Deppe, J.; Friedrichs, G.; Romming, H.-J.; Wagner, H. G. *Phys. Chem. Chem. Phys.* **1999**, *1*, 427.
(39) Votsmeier, M.; Song, S.; Hanson, R. K.; Bowman, C. T. *J. Phys. Chem. A* **1999**, *103*, 1566.
(40) Park, J.; Lin, M. C. *J. Phys. Chem. A* **1999**, *103*, 8906.
(41) Phillips, L. F. *Chem. Phys. Lett.* **1987**, *135*, 269.
(42) Donnelly, V. M.; Baronavski, A. P.; McDonald, J. R. *Chem. Phys.* **1979**, *43*, 271.
(43) Mordaunt, D. H.; Dixon, R. N.; Ashfold, M. N. R. *J. Chem. Phys.* **1996**, *104*, 6472.
(44) Nadtochenko, V. A.; Sarkisov, O. M.; Frolov, M. P.; Tsanava, R. A.; Cheskis, S. G. *Kinet. Katal.* **1982**, *22*, 670.
(45) Halpern, J. B.; Hancock, G.; Lenzi, M.; Welge, K. H. *J. Chem. Phys.* **1975**, *63*, 4808.
(46) Donnelly, V. M.; Baronavski, A. P.; McDonald, J. R. *Chem. Phys.* **1979**, *43*, 283.
(47) Wysong, I. J.; Jeffries, J. B.; Crosley, D. R. *J. Chem. Phys.* **1990**, *93*, 237.
(48) Yamasaki, K.; Tanaka, A.; Watanabe, A.; Yokoyama, K.; Tokue, I. *J. Phys. Chem.* **1995**, *99*, 15086.
(49) Biesner, J.; Schnieder, L.; Ahlers, G.; Xie, X.; Welge, K. H.; Ashfold, M. N. R.; Dixon, R. N. *J. Chem. Phys.* **1989**, *91*, 2901.
(50) Dressler, K.; Ramsay, D. A. *Philos. Trans. R. Soc. A* **1959**, *251*, 553.
(51) Johns, J. W. C.; Ramsay, D. A.; Ross, S. C. *Can. J. Phys.* **1976**, *54*, 1804.
(52) Vervloet, M.; M.-Lafore, M. F.; Ramsay, D. A. *Chem. Phys. Lett.* **1978**, *57*, 5.
(53) Kawaguchi, K.; Yamada, C.; Hirota, E.; Brown, J. M.; Buttenshaw, J.; Parent, C. R.; Sears, T. *J. Mol. Spectrosc.* **1980**, *81*, 60.
(54) Burkholder, J. B.; Howard, C. J.; McKellar, A. R. W. *J. Mol. Spectrosc.* **1988**, *127*, 415.
(55) Ross, S. C.; Birss, F. W.; Vervloet, M.; Ramsay, D. A. *J. Mol. Spectrosc.* **1988**, *129*, 436.
(56) Sarkisov, O. M.; Umanskii, S. Y.; Cheskis, S. G. *Dokl. Russ. Akad. Nauk SSSR* **1979**, *246*, 662.
(57) Xiang, T.-X.; Gericke, K.-H.; Torres, L. M.; Guillory, W. A. *Chem. Phys.* **1986**, *101*, 157.
(58) Chichinin, A. I.; Krasnoperov, L. N. *Chem. Phys. Lett.* **1985**, *115*, 343.
(59) Xiang, T.-X.; Torres, L. M.; Guillory, W. A. *J. Chem. Phys.* **1985**, *83*, 1623.
(60) Benson, S. W. *The Foundation of Chemical Kinetics*; Robert E. Krieger Publishing: Malarbar, FL, 1982.
(61) Jacox, M. E. *J. Phys. Chem. Ref. Data* **1988**, *17*, 269.
(62) Shimanouchi, T. Molecular Vibrational Frequencies. In NIST Chemistry WebBook, NIST Standard Reference Database Number 69; Mallard, W. G., Linstrom, P. J., Eds.; February 2000, National Institute of Standards and Technology, Gaithersburg MD, 20899 (http://webbook.nist.gov).
(63) Stothard, N.; Humpfer, R.; Grotheer, H.-H. *Chem. Phys. Lett.* **1995**, *240*, 474.
(64) Salzman, J. D.; Bair, E. J. *J. Chem. Phys.* **1964**, *41*, 3654.
(65) Lozovskii, V. A.; Nadtochenko, V. A.; Sarkisov, O. M.; Cheskis, S. G. *Kinet. Katal.* **1979**, *20*, 918.
(66) Howard, C. J. *J. Phys. Chem.* **1979**, *83*, 3.
(67) Dorthe, G.; Caubet, Ph.; Vias, Th.; Barrere, B.; Marchais, J. *J. Phys. Chem.* **1991**, *95*, 5109.
(68) Davidson, D. F.; K.-Hoinghaus, K.; Chang, A. Y.; Hanson, R. K. *Int. J. Chem. Kinet.* **1990**, *22*, 513.
(69) Carbaugh, D. C.; Munno, F. J.; Marchello, J. M. *J. Chem. Phys.* **1967**, *47*, 5211.
(70) Dransfeld, P.; Hack, W.; Kurzke, H.; Temps, F.; Wagner, H. G. *Symp. Int. Combust. Proc.* **1985**, *20*, 655.
(71) Xu, Z.-F.; Fang, D.-C.; Fu, X.-Y. *Int. J. Quantum Chem.* **1998**, *70*, 321.
(72) Yardley, J. T. *Intramolecular Energy Transfer*; Academic Press: New York, 1980.